J|A|C|S COMMUNICATIONS

Published on Web 10/06/2009

Synthesis of ZnO Hexagonal Single-Crystal Slices with Predominant (0001) and (000$\bar{1}$) Facets by Poly(ethylene glycol)-Assisted Chemical Bath Deposition

Xiaoheng Liu,[†,‡] Mohammad Afzaal,[†] Karthik Ramasamy,[†] Paul O'Brien,[*,†] and Javeed Akhtar[†]

School of Chemistry and School of Materials, The University of Manchester, Oxford Road, Manchester M13 9PL, U.K., and Key Laboratory for Soft Chemistry and Functional Materials, Ministry of Education, Nanjing University of Science and Technology, Nanjing 210094, China

Received August 19, 2009; E-mail: paul.obrien@manchester.ac.uk

The preparation and properties of metal oxides with highly reactive facets has, of late, received considerable attention.[1] Useful examples, such as microcrystals of anatase (TiO_2) with a large percentage of (0001) facets, have been reported. Zinc oxide nano/microstructures often have interesting physical or chemical properties for optical,[2] electronic,[3] catalytic,[4] or sensing[5] applications. In many cases, hexagonal crystals are expressed with both polar and nonpolar facets. The former are usually either Zn-terminated [the (0001) facet] or O-terminated [the (000$\bar{1}$) facet]. The nonpolar facets are the (10$\bar{1}$0), ($\bar{1}$010), (1$\bar{1}$00), ($\bar{1}$100), (0$\bar{1}$10), and (01$\bar{1}$0) facets. In such structures, the polar surfaces (the ones with potentially high activity) are often relatively diminished as crystal growth progresses. In one sense, this is a fundamental problem resulting from the minimization of surface energy.[1,6] The rod morphology often seen for ZnO nanoparticles is due to growth prevailing along the [0001] direction of a hexagonal single crystal. However, the (0001) and (000$\bar{1}$) facets of the hexagonal ZnO single crystals have particular and specific catalytic activities in some important chemical reactions, such as adsorption of CO on ZnO surfaces during the synthesis of methanol.[4]

Much of our work has focused on the controlled growth of crystals, including those of ZnO.[7] In general, a low percentage of the (0001) and (000$\bar{1}$) facets are seen on ZnO nano- or microcrystalline rods. If a ZnO crystal rod is cut into many shorter cylinders or disks, the relatve amounts of (0001) and (000$\bar{1}$) facets present in a sample increase.

Chemical bath deposition (CBD) has the advantages of low-cost, low-temperature operation and use of aqueous chemistry.[7,8] CBD has been extensively used for the deposition of ZnO films onto glass, silicon, plastic, and other substrates.[3,7,9] It can generate different controllable morphologies (shape, size, and packing of ZnO particles) depending on the precise conditions of deposition. Besides rods in vertical or other alignments, ZnO crystallites such as hexagons, spheres, stars, helices, and other types have been reported. The morphology of the ZnO films is largely dependent on the deposition conditions, ligand, stabilizer, pH value, metal counterion, ionic strength, reaction time, reaction temperature, crystal growth seed, and substrate. Hexamethylenetetramine, citrate, ethylenediamine, triethanolamine, and other small organic molecules have been successfully used as the CBD ligand or stabilizer.[7,9]

Relatively little work has been reported on ZnO films produced by CBD with polymers as the stabilizer, but different polymers have been extensively used in the fabrication of nanomaterials.[10] We[11] and other groups[12] have found that poly(ethylene glycol) (PEG) is a good choice for the microstructural control of inorganic nanomaterials. In the present work, we used PEG to modify the deposition of thin films by CBD. This approach leads to shorter cylinders or disks consisting of many separable slices with an extremely large surface of (0001) and (000$\bar{1}$) facets (Scheme 1).

Scheme 1. Illustration of a ZnO Rod That Has Its Predominant Growth Direction along [0001] but Has Been Cut into Shorter Cylinders and Then into Thinner Slices (A ZnO Short Cylinder or Disk Consisted of Thinner Hexagonal Single Crystal Slices, and This Particle Was Easily Converted into Free Slices through the Use of PEG as the Stabilizer)

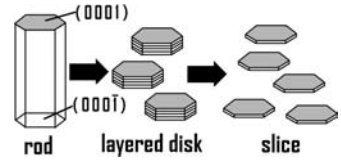

In a recent and related CBD deposition, a water/alcohol mixed solvent was used to form ZnO microdisks,[13] which may reflect an interaction between Zn(II) and the alcohol O atom. In the present study, we chose PEG as an adjunct reagent in CBD, not only using its O atoms to interact with Zn(II) but also using the stabilization of the PEG macromolecular chain. This yielded a product with better, flatter lamellar morphologies.

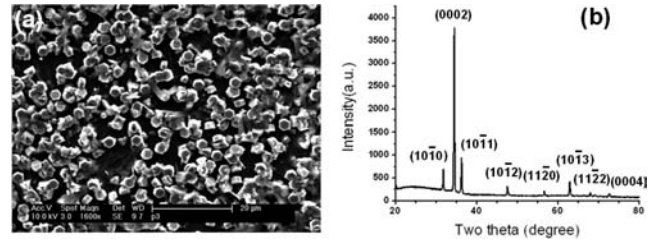

Figure 1. (a) FESEM image of thin film consisting of discrete cake-like ZnO particles (scale bar: 20 μm). (b) XRD pattern of a ZnO film fabricated by PEG-assisted CBD.

The as-grown ZnO film was of high quality (Figure 1a). Most of the material composing the film was homogeneous, with a predominance of short hexagonal cylinders or disks with a longest dimension of ~3 μm (Figure 2a and Figure S2 in the Supporting Information). The thickness of the crystallites was ~1.27 μm (see the Supporting Information). The as-fabricated thin film was characterized by X-ray diffraction (XRD), as shown in Figure 1b. Several sharp Bragg peaks were observed, in good agreement with the wurtzitic form of ZnO (hexagonal phase, space group $P6_3mc$, ICDD No. 36-1451). The calculated hexagonal cell values (a = 3.247 Å, c = 5.210 Å) are in good agreement with those of ICDD No. 36-1451 (a = 3.250 Å, c = 5.207 Å). The strongest (0002) reflection is typical of a rodlike morphology and [0001]-oriented rods. This reflects the structure shown in the field-effect scanning electron microscopy (FESEM) image, with flattish hexagons largely resting on the substrate (Figure 1a). The short rods are sufficiently thick for the relative intensities to reflect this orientation.

FESEM images showed that the particles in the film have a "cakelike" structure (Figure 2a). Transmission electron microscopy

[†] The University of Manchester.
[‡] Nanjing University of Science and Technology.

10.1021/ja906992s CCC: $40.75

(TEM) studies (Figures 2b,c and 3a and Figure S3) indicated that the cakelike ZnO particles actually consist of layered slices. Although this layer-by-layer structure in ZnO crystals has been seen previously,[14] here we demonstrate that this layer-by-layer structure can be further separated into slices using a simple method, ultrasonication in ethanol. Figure 2b shows layer-by-layer aggregation, and more clearly, two layers (at least) of aggregation can be seen in Figure 2c. Quantitative energy-dispersive X-ray analysis (EDX) obtained from several crystals revealed a Zn/O ratio of 1:1, within the error of EDX.

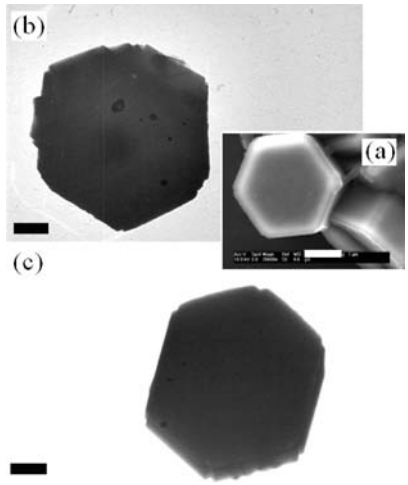

Figure 2. (a) FESEM image of magnified cakelike ZnO particles in the film (scale bar: 1 μm). (b, c) TEM images of layer-by-layer structure in a cakelike ZnO particle (scale bar: 0.5 μm).

There are some transparent ZnO slice fragments in Figure 3a, as compared with the ZnO slices in Figure 2b,c; these fragments may be formed directly from the crystal growth, or the original slices of the fragments are thinner and may be easily damaged in ultrasonication. However, there are still large numbers of (0001) and (000$\bar{1}$) facets for these fragments. The thickness of these transparent slices was estimated to be 100 nm by TEM. Both the slices and the fragments in Figures 2 and 3 and Figure S3 present the same electron diffraction (ED) patterns (Figure S4). This suggests that they are good single crystals.

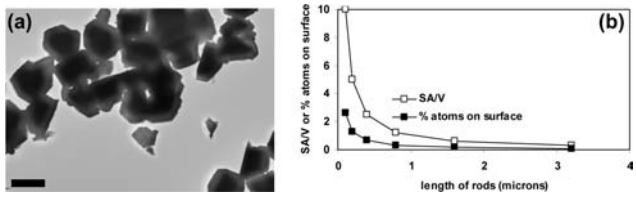

Figure 3. (a) TEM image of transparent ZnO slice fragments (scale bar: 2 μm). (b) Plot showing the changes in the percentage of surface atoms (■) and surface area/volume ratio (□).

We previously reported algorithms for calculating the number of atoms in perfect crystals of various sizes.[6] It is interesting to apply a slight modification of this approach to the present system to assess the potential significance and or usefulness of any changes in surface area. We developed calculations of the number of atoms in perfect single crystals and applied them to this system. Figure 3b shows the variation in the total surface area divided by the volume for a 3.2 $\times$ 1.5 μm (height by edge length) rod as it is divided binomially into 2, 4, 8, 16, and 32 slices, at which point the height of a slice is 100 nm. The second plot is the percentage of atoms on the surfaces, which varies in the same manner as the first. An individual rod starts with 1.28×10^8 atoms on (0001)-type faces but in 100 nm slices has 4.1 $\times 10^9$ such atoms on (0001) type faces, a change from 0.08 to 2.6% of the atoms. These simple calculations show the potential of such materials to provide crystals with large numbers of active sites (e.g., for catalysis).

Morphological control in the growth of ZnO nanostructures, including disk and hierarchical ZnO nanostructures, has been reported extensively.[13−15] In contrast to previous studies on disklike and hierarchical ZnO nanostructures, we have carried out systematic research to enlarge the relative area of (0001) and (000$\bar{1}$) facets via chemical methods by means of PEG fragmentation. Furthermore, the subunits in the particles are easily turned into free material and consist of hexagonal single-crystal slices with an extremely large relative surface area of (0001) and (000$\bar{1}$) facets. This research based on a simple chemical process (PEG-assisted CBD) establishes a pathway for obtaining highly active ZnO catalysts and other functional materials, which depend largely on the (0001) or (000$\bar{1}$) facets of ZnO.

Acknowledgment. This work was supported by EPSRC (U.K.). X.L. thanks the NSFC (50772048) and CSC (China).

Supporting Information Available: Experimental details and additional figures, including a digital photo, additional SEM and TEM images, and an ED pattern of ZnO samples. This material is available free of charge via the Internet at http://pubs.acs.org.

References

(1) (a) Yang, H. G.; Sun, C. H.; Qiao, S. Z.; Zou, J.; Liu, G.; Smith, S. C.; Cheng, H. M.; Lu, G. Q. *Nature* **2008**, *453*, 638. (b) Xie, X. W.; Li, Y.; Liu, Z. Q.; Haruta, M.; Shen, W. J. *Nature* **2009**, *458*, 746.
(2) (a) Malandrino, G.; Blandino, M.; Fragala, M. E.; Losurdo, M.; Bruno, G. *J. Phys. Chem. C* **2008**, *112*, 9595. (b) Li, H. D.; Yu, S. F.; Lau, S. P.; Leong, E. S. P.; Yang, H. Y.; Chen, T. P.; Abiyasa, A. P.; Ng, C. Y. *Adv. Mater.* **2006**, *18*, 771.
(3) (a) Wang, Z. L.; Song, J. H. *Science* **2006**, *312*, 242. (b) Greene, L. E.; Law, M.; Tan, D. H.; Montano, M.; Goldberger, J.; Somorjai, G.; Yang, P. *Nano Lett.* **2005**, *5*, 1231.
(4) (a) Kurtz, M.; Strunk, J.; Hinrichsen, O.; Muhler, M.; Fink, K.; Meyer, B.; Wöll, C. *Angew. Chem., Int. Ed.* **2005**, *44*, 2790. (b) Wöll, C. *Prog. Surf. Sci.* **2007**, *82*, 55.
(5) (a) Trivikrama Rao, G. S.; Tarakarama Rao, D. *Sens. Actuators, B* **1999**, *55*, 166. (b) Chu, X.; Jiang, D.; Djurisic, A. B.; Leung, Y. H. *Chem. Phys. Lett.* **2005**, *401*, 426.
(6) Thomas, P. J.; O'Brien, P. *J. Am. Chem. Soc.* **2006**, *128*, 5614.
(7) (a) Govender, K.; Boyle, D. S.; O'Brien, P.; Binks, D.; West, D.; Coleman, D. *Adv. Mater.* **2002**, *14*, 1221. (b) Govender, K.; Boyle, D. S.; Kenway, P. B.; O'Brien, P. *J. Mater. Chem.* **2004**, *14*, 2575.
(8) Hodes, G. *Chemical Solution Deposition of Semiconductor Films*; Marcel Dekker: New York, 2003.
(9) (a) Vayssieres, L. *Adv. Mater.* **2003**, *15*, 464. (b) Cheng, H.-C.; Chen, C.-F.; Tsay, C.-Y. *Appl. Phys. Lett.* **2007**, *90*, 012113. (c) Liu, B.; Zeng, H. C. *Langmuir* **2004**, *20*, 4196. (d) Sounart, T. L.; Liu, J.; Voigt, J. A.; Hsu, J. W. P.; Spoerke, E. D.; Tian, Z. R.; Jiang, Y. B. *Adv. Funct. Mater.* **2006**, *16*, 335. (e) Yan, X. D.; Li, Z. W.; Chen, R. Q.; Gao, W. *Cryst. Growth Des.* **2008**, *8*, 2406. (f) Kokotov, M.; Hodes, G. *J. Mater. Chem.* **2009**, *19*, 3847.
(10) (a) Cushing, B. L.; Kolesnichenko, V. L.; O'Connor, C. J. *Chem. Rev.* **2004**, *104*, 3893. (b) Laurent, S.; Forge, D.; Port, M.; Roch, A.; Robic, C.; Vander Elst, L.; Muller, R. N. *Chem. Rev.* **2008**, *108*, 2064.
(11) Liu, X. H.; Yang, J.; Wang, L.; Yang, Y. J.; Lu, L. D.; Wang, X. *Mater. Sci. Eng., A* **2000**, *289*, 241.
(12) (a) Zhou, X. F.; Zhang, D. Y.; Zhu, Y.; Shen, Y. Q.; Guo, X. F.; Ding, W. P.; Chen, Y. *J. Phys. Chem. B* **2006**, *110*, 25734. (b) Devi, G. S.; Hyodo, T.; Shimizu, Y.; Egashira, M. *Sens. Actuators, B* **2002**, *87*, 122.
(13) Wang, M. S.; Kim, E. J.; Hahn, S. H.; Park, C. H.; Koo, K. K. *Cryst. Growth Des.* **2008**, *8*, 501.
(14) Zhang, R.; Kumar, S.; Zou, S. Z.; Kerr, L. L. *Cryst. Growth Des.* **2008**, *8*, 381.
(15) (a) Pan, Z. W.; Budai, J. D.; Dai, Z. R.; Liu, W. J.; Paranthaman, M. P.; Dai, S. *Adv. Mater.* **2009**, *21*, 890. (b) Cole, J. J.; Wang, X. Y.; Knuesel, R. J.; Jacobs, H. O. *Nano Lett.* **2008**, *8*, 1477. (c) Kuo, C. L.; Kuo, T. J.; Huang, M. H. *J. Phys. Chem. B* **2005**, *109*, 20115. (d) Chang, Y. C.; Yang, W. C.; Chang, C. M.; Hsu, P. C.; Chen, L. J. *Cryst. Growth Des.* **2009**, *9*, 3161. (e) Tian, Z. R.; Voigt, J. A.; Liu, J.; Mckenzie, B.; Mcdermott, M. J. *J. Am. Chem. Soc.* **2002**, *124*, 12954. (f) Xu, C. X.; Sun, X. W.; Dong, Z. L.; Cui, Y. P.; Wang, B. P. *Cryst. Growth Des.* **2007**, *7*, 541. (g) Xu, F.; Lu, Y. N.; Xie, Y.; Liu, Y. F. *J. Phys. Chem. C* **2009**, *113*, 1052. (h) Yoshida, T.; Tochimoto, M.; Schlettwein, D.; Wöhrle, D.; Sugiura, T.; Minoura, H. *Chem. Mater.* **1999**, *11*, 2657.

JA906992S